

HIERARCHICALLY POROUS GRAPHENE IN NATURAL GRAPHITIC GLOBULES FROM SILICATE MAGMATIC ROCKS

V. A. Ponomarchuk^{1,2}, A. T. Titov^{1,2}, T. N. Moroz¹, A. N. Pyrayev¹, A. V. Ponomarchuk¹

¹Sobolev Institute of Geology and Mineralogy SB RAS, Novosibirsk, Russia

²Novosibirsk State University, Novosibirsk, Russia

ponomar@igm.nsc.ru, pyrayev@gmail.com

PACS 81.00.00 + 81.05.ue + 83.80.Nb

Naturally-occurring nanostructured graphites from silicate magmatic rocks, which are rare, were characterized using electron microscope and X-ray spectroscopy. This graphite consists of porous carbon, nanographite layers, micro- and nanotubes. The porous carbon is classified as macroporous matter with a small amount of mezopores. Evidence for the unusual properties of porous carbon are given: nanographite layers are created at the exposed surface of sample and the nanotubes occurs in the bulk of porous carbon.

Keywords: Porous carbon, Nature nanostructured graphite, Graphene, Microtubes, Nanotubes, Magmatic rock.

1. Introduction

Over the past 30 years the understanding about the properties of carbon has increased considerably, due to the study of fundamental physical and chemical properties of laboratory-produced synthetic nanomaterials. Thus, along with well-known allotropic forms of condensed carbon, allotropes with zero dimensionality (0-D) - fullerene [1], graphene (2-D-allotrope), micro- and nanotubes (1-D-allotrope) [2] have been discovered. It should be noted, relative to the last allotrope, that pioneer investigations of 1-D-structures were published in 1952 [3] by domestic (Russian) inventors. The publications mentioned above have attracted an enormous amount of attention from the scientific community, as expressed by an increased number of theoretical and experimental investigations, searching of nanotechnology-based solutions, synthetic methods for different carbon morphologies and organized assemblies of them. In addition, the emphasis for research of sp^2 -connected carbon nanostructures has changed direction over time, from fullerene followed by nanotubes to graphene and porous carbon. Porous carbon is used for battery electrodes, catalyst supports, supercapacitors, immobilization of biomolecules as well as adsorption agent of molecules in liquid phase, in water purification processes. The last usage is an old one, dating to 2000 B.C. in ancient Egypt at that [4]. However, the exclusive properties of porous carbon are not limited to the above-mentioned range of applications. In this paper, based on phenomenological data about natural graphite extracted from magmatic rock, we report here about porous carbon as a basic element that combines 1D and 2D nanostructures in 3D-superstructures.

The synthesis of sp^2 -hybridized carbon nano- and microstructures is carried out in both laboratory and industrial scale setups. Although numerous reviews [5, 6, 7, 8 et al.] display widely varying synthetic methods, all have a common conceptual design consisting of: heating (plasma, laser, microwaves, electric arc, thermal heating), carbon-bearing precursor

(methane, acetylene etc.), commonly presence of metal catalysts (Fe, Ni, Co etc.), relatively short experiment time (ranged between minutes and tens of hours) and severely controlled timing.

Generally, artificial synthesis of carbon nanostructures is carried out under low pressure conditions (less than atmospheric pressure). A few works [9] report details about high-pressure (500 MPa) synthesis of such carbon nanostructures. These facts indicate the wide range of acceptable pressures to form carbon nanostructures.

It is unlikely that all these “man-made” conditions are fulfilled in a natural environment. Single cases of sp^2 -hybridized carbon nano- and microstructures are detected in geological samples [10], thus confirming the partial appearance of the above-mentioned factors required for synthesis in combination with currently unknown “natural” nanotechnology specificities. Identifying of these specificities is a very important problem and a solution to this problem demanded primarily investigation of natural sp^2 -hybridized carbon structures (microtubes, porous carbon, graphene and nanographite layers) and combinations thereof.

2. Materials and methods

The exotic needle-shaped form of graphite was first discovered and described in the graphite-palagonit globular leukogabbro of Verhnetalnahskaya stratified trap intrusions in the Siberian platform [11]. The amount of graphite in leukogabbro reaches 3-5%. Graphite occurs in the form of globules in rock. The size of the globules varies from 0.5 mm to 1.5–2 cm. Under the microscope, small globules have the shape of a sphere or an ellipsoid, while large globules have an amoeba-shaped form. The morphology of globules is determined by the fringe of dense graphite on its periphery. The outer surface of each globule is smooth, while the interior has brush needle-like crystals of graphite. In the central parts of multi-layer graphite globules, needle accretions of graphite in the form of a sea urchin are found. Mesostasis in the graphite globules is presented by palagonite, amphibole, clinopyroxene, ilmenite and apatite. This paper presents data on the morphological features of natural carbon aggregation and micro- and nano-carbon structures.

In order to investigate in detail the morphology, texture and structure of graphite particles, they were separated from a silicate rock by numerous “soft” decomposition of samples in hydrofluoric acid followed by hand sampling and an additional chemical purification process. Initially, graphite particles remain in rocks until, under stressed conditions, they are removed by rock decomposition. The graphite materials under investigation, therefore, occur as individual fragments.

The obtained samples were characterized using the following: optical microscope, scanning electron microscopy TSCAN and X-ray microprobe analysis with the energy (EDX) and wave (WDX) dispersion (LEO1430VP equipped with EDX OXFORD and MEBAX-micro), Jobin Ivon Raman spectrometer T6400 (excitation radiation $\lambda = 514.5$ nm, Ar+laser) equipped with optical microscope and Finnigan MAT-253 mass spectrometer equipped with Elemental Analyser EA 1112 and GasBench II (the precision is $\pm 0.2\%$).

3. The structure and morphology of nanostructured assembly

The series of scan-images (figures below) make possible the detailed study of the structure, texture and morphology of the inner and outer parts of different graphite particle fragments of graphite particles. Graphite particles characterized by 3D-regularity are composites consisting of elementary nanostructures: nano- and microtubes (1D-regularity), nanographite layers (2D-regularity) and porous carbon. These structures have a certain order with regards to each other as shown in scan-image of globule (fig. 1A and 1B).

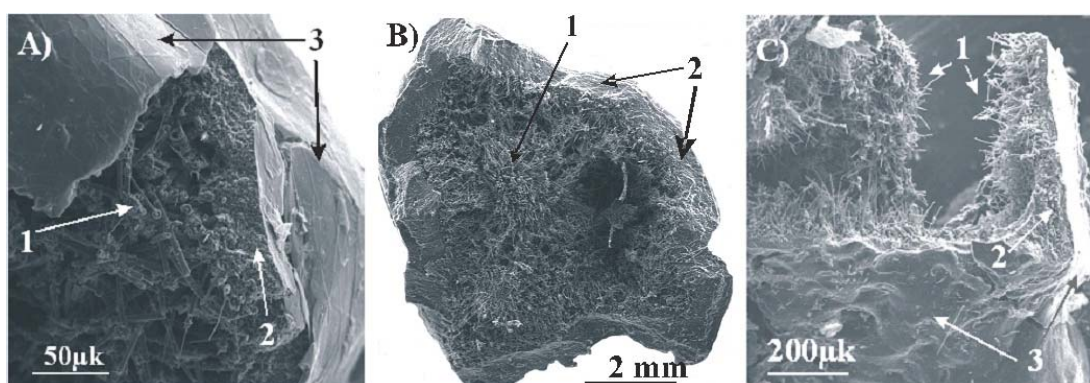


FIG. 1. Scan-image of nature nanostructured graphite fragments: A) – globule, B) – crust, C) fragment of nanostructured graphite. Symbolic notations: **1** – micro- and nanotubes; **2** – porous carbon; **3** – wrinkle nanographite layer

Outer surface (**3**), an organized nanographite layer, is the boundary surface between a rock and graphite particle. The surface morphologies of the graphite formations under investigation here are given in detail in [12]. Here, it should be noted that the cleavage (“wrinkle”) character of a particle surface is usually explained by a difference in the thermal expansion coefficients of nanographite and the carrier rock.

There is a contact between nanographite layer and porous carbon in the inner part (**2**). Micro- and nanotubes “grow out” of porous carbon, as shown in fig. 1A and 1B. This is a typical phenomenon in studied natural nanostructured graphites. The series of scan-images (figure 2) illustrate graphite particle portions- porous carbon - micro- and nanotubes and makes their relationship more clear. Figure 2A exhibits a scan-image of a planar graphite particle covered by a micro- and nanotubes “forest” on the one side (about 500 tubes per square mm) and nanographite layer on the other side (not shown in the figure). Porous carbon is situated between the microtube base and nanographite layer. The appearance of a secondary nanographite layer (**3**), situated over micro- and nanotubes, is a feature of this sample. On the basis of microscopic observations, it may be concluded that this layer was extended along the full surface of planar structure, but only a part of it remains after sample preparation procedures.

Radial structures **4** (fig. 2A), composed of small porous carbon round sectors and radially extended multilayer nano- and microtubes (fig. 2B) attract special interest. The existence of such structural combinations indicated a feature of “natural” nanotechnology not previously mentioned in the literature relating to the laboratory synthesis of nanostructures, as far as we know. Structural binding of porous carbon and nano- and microtubes is an important element of the natural nano- and microtube formation model.

There are cylindrical hollow tubes **5** (fig. 2B) in the central part of porous carbon round islands (**4**, fig. 2A). It should be mentioned that hollow tubes with diameters varying from units to tens of microns were observed in porous carbon layers of natural nanostructured graphite. This can be considered as fluid and solution conductors [12, 13]. The walls of the hollow tubes are nanographite layers **7** (fig. 3A). The formation of fluid-conducting tubes with nanographite incrustation in porous carbon is an unusual fact that undoubtedly attracts the attention of nanotechnology investigators because of the realization of a graphene synthetic method different from previously known techniques [14].

The data described above exhibit quite a constructive role for porous carbon, due to its properties in naturally nanostructured graphite formation process. The properties of

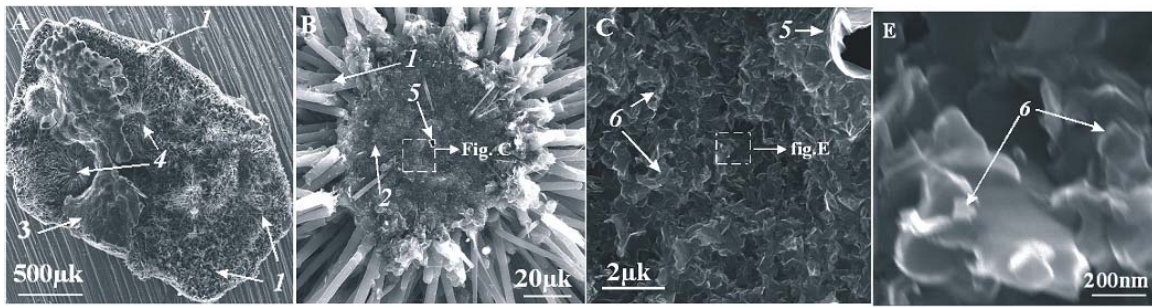


FIG. 2. Scan-image of flat nanostructured graphite fragment. A – overview; B – fluid-conducting canal within the frame of the porous graphite and radially expanded micro- and nanotubes; C – porous graphite surface - multiplied image of square dashed line sector of fig. 2B; E – porous graphite surface - multiplied image of square dashed line sector of fig. 2C. Symbolic notations: (1, 2, 3 - look at fig. 1), 4 – porous carbon round islands, 5 – fluid-conducting cylindrical hollow tube, 6 – fragments of nanographite layers

porous carbon can be partially revealed from the scan-images series shown in fig. 2B, 2C and 2E. It is obvious that porous carbon consists of numerous disorderly linked wrinkle fragments of nanographite layers. There is a strong linking between fragments of nanographite layers plane and nanographite sheet borders due to their chemical activity. It is impossible to estimate the pore size of samples under investigation quantitatively, but it is possible using visual evaluation of fig. 2C and 2E to distinguish sufficiently large pores (around 50 nm) that are attributed to the porous and macroporous (i.e. multimodal) materials, according to supposition of Dubinin [15], which was subsequently accepted by IUPAC [16].

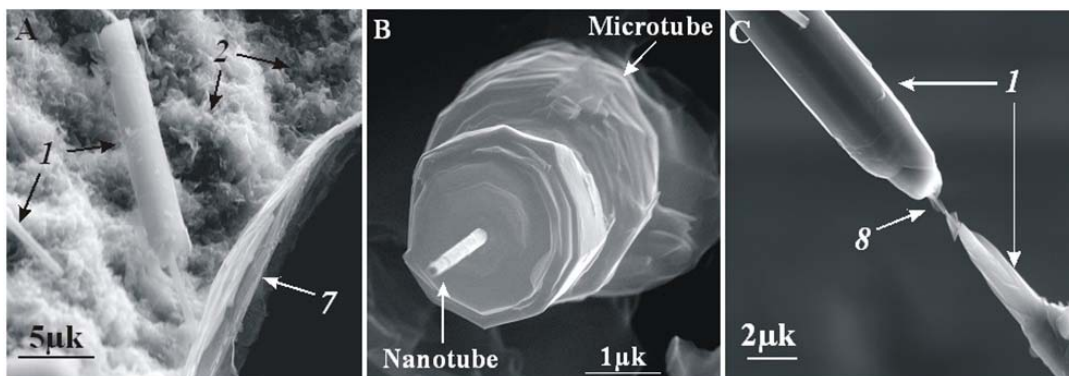


FIG. 3. A – scan-image of complex combination of the fluid-conducting canal, porous carbon, micro- and nanotube and wall of fluid-conducting canal composed of nanographite layer; B – nanotube wrapped in microtube; C – microtubes linked by nanotube. The microtube helix is due to chirality

Along with porous carbon, an easily-discernible nanotube with diameter of about 100 nm or less wrapped in a segment of microtube is shown in fig. 3A. The nanotube is located along the axis line of microtube. Such a complex combination of micro- and nanotubes is the most that natural specimens feature as may be seen in the numerous scan-images. There are three interesting features in this picture: 1 – microtubes (with the diameter more than 100 nm) were more subject to destruction than nanotubes. This point can be explained by the expanded linear size of nanotubes in comparison with microtubes

that are illustrated by fig. 3B and 3C. The stated interpretation is in accordance with the nano-physical data: strength increases with decreasing linear size; 2 – the 100 nm limit, in this case, is a natural border for the 1-dimensional carbon structure, mechanical properties exchange, as well as an amazing border that divides the nano-world from the micro-world [17]; 3 – there is a difference between the nano- and microtube interaction with porous carbon, as is clearly shown in fig. 2B. The base of the microtubes only contact the porous carbon, while nanotubes penetrate into the porous carbon. In spite of the morphological unity of micro- and nanotubes, the last point indicates that there are different formation mechanisms for each of these structures.

The formation of nanotubes is quite acceptably explained by a vapor–liquid–solid (VLS) mechanism [18]. The main points of VLS-mechanism are the decomposition of carbon-bearing phase in the raw material, diffusion of elemental carbon to metallic catalyst, saturation of the catalyst surface by carbon and structurization of nanotube. The component composition of nanostructured graphite was investigated using EDC and SR XRF [13]. It exhibits a relatively high content of Fe in carbon matrix, reaching 2 wt. %. The SR XRF data showed the presence of platinum (~ 10 ppm) in studied nanostructured graphites, as well as the Fe catalyst of the VLS-mechanism and is able to initiate nanotube formation. Subsequent increasing of the nanotube radius may be conceptually explained by another mechanism: carbon deposition according to vapor-grown carbon fibers (VGCF) model [19]. Many of the process details for this model must be specified. In order to understand the mechanism of porous carbon formation, additional investigations are necessary.

In addition to electron microscopy and elemental analysis, the natural nanostructured graphite was characterized by Raman spectroscopy. This widely-applicable method has been used recently to characterize graphite formations (including different nanostructures such as nanographite ribbons, carbon nanotubes and fullerenes [20]). It should be noted that since this is a non-destructive analysis, the same specimen may be used in subsequent analyses. Moreover, it is even possible to estimate the temperature of graphite formation in geological objects using Raman spectroscopy [21].

The recording of the signal was conducted using a multi-channel detector with backscattering geometry and an unconditioned orientation of the sample. Figure 4 shows examples of typical Raman spectra for observable nanostructured graphites. There are three significant peaks in these spectra. The Raman peak at 1580 cm^{-1} , referred to first order spectrum, is specified by a one-background process of Raman dispersion and is due to a doubly-degenerate symmetry component E_{2g} of the Brillouin zone. This band is always present in graphite spectra and marked as G . Simultaneously, it should be noted that this band is typical in all spectra of sp^2 -hybridized carbon compounds.

The Raman band at 1352 cm^{-1} , marked in fig. 4 as D_1 , is usually explained by the presence of defects in the sample, and in the case of grapheme, by boundary defects, such as ragged carbon bonds. While the D_1 peak is quite intense there is a low intensity peak D_2 , appearing at the long wavelength end of peak G . Substantially, peak D_2 should be considered as a “shoulder” of the G peak. The spectra of highly-oriented pyrolytic graphite (HOPG) exhibit a low intensity of peak D_1 in comparison with peak G . This is considered as a criterion of significant graphite crystallite grain size. The table demonstrates relations $R_1 = D_1/G$ of the investigated graphites. The R_1 values range from 0.02 to 0.2, seemingly indicating a high level of graphite crystallinity.

In order to quantitatively evaluate the degree of crystallinity for carbonaceous matter using Raman spectra data, the formalism depicted in [21] was used. Calculation were performed using the relation $R_2 = I_{D1}/(I_G + I_{D1} + I_{D2})$, where I_G , I_{D1} and I_{D2} — are squares

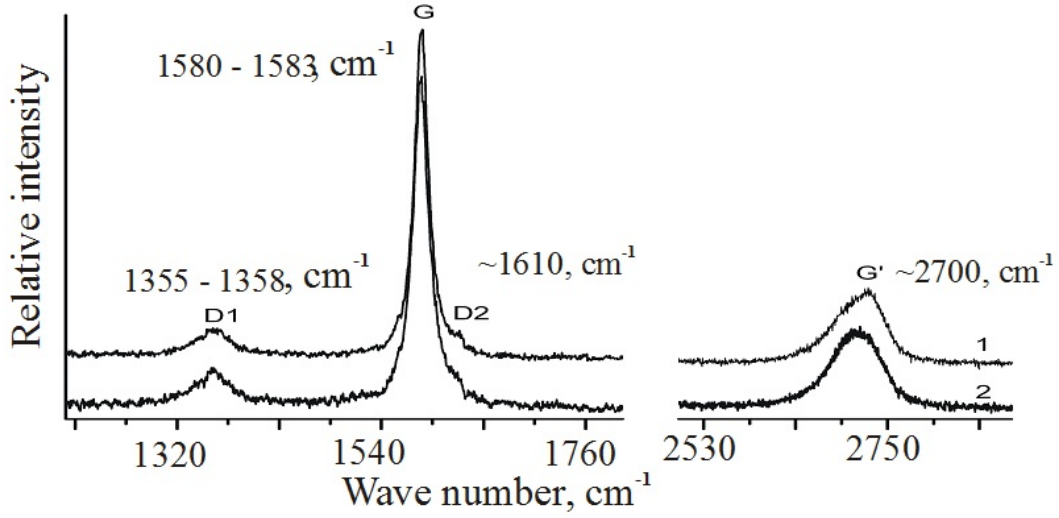


FIG. 4. Raman spectra of nature nanostructured graphites

TABLE 1. Raman spectra parameters of nanostructured graphites from magmatic rocks

	R_2	R_1	Peak position D_1 (cm^{-1})	Peak D_1 width (cm^{-1})	Peak position G (cm^{-1})	Peak G width (cm^{-1})	Crystallite size L_a (\AA)
nt1	0.0408	0.024	1359.8	26.9	1583.0	15.29	~ 2000
nt2	0.1916	0.08	1358.3	53.1	1583.1	17.77	~ 230
nt3	0.2385	0.107	1357.0	66.4	1582.3	20.32	129
nt4	0.3069	0.186	1355.6	64.9	1580.2	24.51	96

of G -, D_1 - and D_2 -peaks accordingly. The table presents that as R_2 increases, the full width at half-height for the D_1 and G peaks increase, as well as the in-plane crystallite size L_a . It is notable that the least defective sample with minimal R_1 value had a significant crystallite size that may be found in HOPG graphites [22]. There is a peak at 2700 cm^{-1} in the short-wave end of the Raman spectrum for the sample. In the case of Bernal's packing and low number of layers (less than 10), the parameters for this peak (position, intensity, peak form) are currently widely used in the characterization of nanostructured carbon as well as in the estimation for the number of graphene layers. This peak in the upper spectrum of fig. 4 is not symmetrical and it is similar in form to graphite. The bottom spectrum, on the basis of numerous publications, apparently demonstrates the occurrence of a significant number of nanographite layers in a sample (more than 10). The temperatures for graphite globules formation, calculated using a previously-reported method [21], indicated a range from 470 to 700°C . Moreover, geological data allows one to estimate the pressure of formation for graphite globules (about 100 – 200 MPa), which is less than the formation pressures for artificial carbon nanostructures [9].

4. Conclusion

The results presented in this paper demonstrate that 3D-graphite formation occurs under exclusive geological conditions. These unique structures consist of porous carbon and sp^2 -like hybridized carbon nanostructures (micro- and nanotubes). The porous carbon is the

key structure of nanostructured graphite because: 1 - nanographite layer formation occurs at the surface of the porous carbon; 2 - nanotube formation occurs within the porous carbon.

References

- [1] H.W. Kroto, J.R. Heath, S.C. O'Brien, R.F. Curl, R.E. Smalley. C60: Buckminsterfullerene. *Nature*, **318**, P. 162 (1985).
- [2] S. Iijima. Helical microtubules of graphitic carbon. *Nature*, **354**, P. 56–58 (1991).
- [3] L.V. Radushkevich, V.M. Lukyanovich. The structure of carbon formed by thermal decomposition of carbon oxide on an iron contact. *Journal of Physical Chemistry*, **26**, P. 88–95 (1952).
- [4] S.M. Manocha. Porous carbons. *Sadhana*, **28**, P. 335–348 (2003).
- [5] M. Paradise, T. Goswami. Carbon nanotubes – Production and industrial applications. *Materials and Design*, **28**, P. 1477–1489 (2007).
- [6] Yu.E. Lozovik, A.M. Popov. Formation and growth of carbon nanostructures: fullerenes, nanoparticles, nanotubes and cones. *Phys. Usp*, **40**, P. 717–737 (1997).
- [7] A.V. Eletskii. Carbon nanotubes. *Phys. Usp*, **40**, P. 899–924 (1997).
- [8] G.D. Nessim. Properties, synthesis, and growth mechanisms of carbon nanotubes with special focus on thermal chemical vapor deposition. *Nanoscale*, **2**, P. 1306–1323 (2010).
- [9] S.K. Simakov, A.A. Grafchikov, A.K. Sirotkin, I.A. Drozdova, E.A. Grebenshchikova, A.E. Lapshin. Synthesis of carbon nanotubes and fullerite structures at PT parameters corresponding to natural mineral formation. *Doklady Earth Sciences*, **376**, P. 87–89 (2001).
- [10] J.A. Jaszczak, S. Dimovski, S.A. Hackney. Micro- and nano-scale graphite cones and tubes from Hackman Valley, Kola Peninsula, Russia. *Canad. Mineralogist*, **45**, P. 379–389 (2007).
- [11] V.V. Ryabov, A.J. Shevko, M.P. Gore. *Magmatic formations of Norilsk region. Petrology of the traps. Atlas of igneous rocks*. Nonpareil, Novosibirsk, 408 p. (2000).
- [12] V.V. Ryabov, V.A. Ponomarchuk, A.T. Titov, D.V. Semenova. Micro- and Nanostructures of Carbon in Pt–Low-Sulfide Ores of the Talnakh Deposit (Siberian Platform). *Doklady Earth Sciences*, **446**(2), P. 1193–1196 (2012).
- [13] V.A. Ponomarchuk, Y.P. Kolmogorov, V.V. Ryabov, A.T. Titov, T.N. Moroz, D.V. Semenova, A.N. Pyryaev, A.V. Ponomarchuk. SR XRF Study of Natural Micro- and Nanostructured Carbon from Igneous Rocks. *Bulletin of the Russian Academy of Sciences. Physics*, **77**(2), P. 203–206 (2013).
- [14] M.J. Allen, V.C. Tung, R.B. Kaner. Honeycomb Carbon: A Review of Graphene. *Chem. Rev.*, **110**(1), P. 132–145 (2010).
- [15] M.M. Dubinin. The potential theory of adsorption of gases and vapors for adsorbents with energetically nonuniform surfaces. *Chem Rev.*, **60**, P. 235–241 (1960).
- [16] IUPAC Manual of Symbols and Terminology, Appendix 2, Pt. 1, Colloid and Surface Chemistry. *Pure Appl. Chem.*, **31**, P. 578 (1972).
- [17] H. Gleiter. Nanostructured materials: basic concepts and microstructure. *Acta Materialia*, **48**(1), P. 1–29 (2000).
- [18] R.T.K. Baker. Catalytic growth of carbon filaments. *Carbon*, **27**, P. 315–323 (1989).
- [19] V.Z. Mordkovich. Carbon Nanofibers: A New Ultrahigh-Strength Material for Chemical Technology. *Theoretical Foundations of Chemical Engineering*, **37**(5), P. 429–438 (2003).
- [20] M.A. Pimenta, G. Dresselhaus, M.S. Dresselhaus, L.G. Cancado, A. Jorio, R. Saito. Studying disorder in graphite-based systems by Raman spectroscopy. *Phys.Chem.Chem.Phys.*, **9**, P. 1276–1291 (2007).
- [21] O. Beyssac, B. Goffe, C. Chopin, J.N. Rouzaud. Raman spectra of carbonaceous material in metasediments: a new geothermometer. *J. metamorphic Geol.*, **20**, P. 859–871 (2002).
- [22] S.S. Bukalov, L.A. Mikhalicin, Ya.V. Zubavichus, L.A. Leytis, U.N. Novikov. Structure investigation of graphites and some another sp² carbonic materials using micro-, Raman spectroscopy and X-ray diffraction methods. *Ros. Chem. J.*, **L**(1), P. 83–91 (2006).